

# Sea Ice Identification Using Dual-Polarized Ku-Band Scatterometer Data

Simon H. Yuch, Ronald Kwok, Shu-Hsiang Lou, and Wu-Yang Tsai

Jet Propulsion Laboratory, MS 300-235

California Institute of Technology

4800 Oak Grove Drive, Pasadena, CA 91109, USA

Tel: 818-354 3012, Fax: 818-393-5285

E-mail: simon@malibu.jpl.nasa.gov

**Abstract** This paper describes a classification algorithm using dual-polarized scatterometer measurements to identify the edge of the sea ice cover. The distinct polarization scattering signatures of sea ice and open water are discussed and illustrated with the dual-polarized radar measurements from the Seasat-A scatterometer (SASS). The analysis of SASS data suggests that the ratio of vertical and horizontal polarization backscatter, denoted as the copol ratio, is a useful discriminator of sea ice and open ocean. A simple classification algorithm using the thresholds of the copol ratio and backscatter levels is proposed. The feasibility of this algorithm is demonstrated using the SASS data from the single-sided, dual-polarization mode. The results indicate that the dual-polarized measurements from the NASA scatterometer (NSCAT) can be used to produce routine maps of sea ice extents.

## INTRODUCTION

In this paper, we describe the potential of using dual-polarized scatterometer returns from the polar orbiting satellite to identify the edge of the ice cover. This ice edge could be used to compute the ice extent which is defined as the area enclosed by the outer boundary of the ice pack. The trends in the maxima and minima of the annual ice extents of the Arctic and Antarctic sea ice covers have been suggested as useful indicators of climate change. Recent investigations have been based on the ice extent derived from data collected by the Scanning Multichannel Microwave Radiometer (SMMR) instrument and its Successor, Special Sensor Microwave Imager (SSM/I). We suggest, here that a dual-polarized scatterometer could be used to discriminate sea ice from open water and that a routine ice edge product derived from active 1111-crowave data could provide an interesting complement to the SSM/I estimates.

### SEA ICE/WATER CLASSIFICATION ALGORITHM

#### A. Scattering Signatures of Sea Ice and Open Water

Sea ice consists of freshwater ice, brine, and air bubbles. The salinity, size, shape, and number densities of brine inclusions and air bubbles in the ice layer are strongly

This work was performed under a contract with the National Aeronautics and Space Administration at the Jet Propulsion Laboratory, California Institute of Technology.

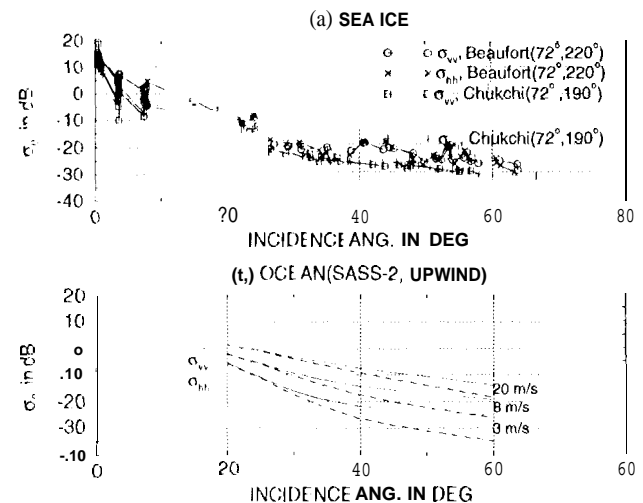


Figure 1. Examples of dual-polarized backscatter data from Seasat scatterometer versus incidence angle. (a) two selected sea ice areas in the Arctic ocean and (b) averaged upwind backscatter coefficients of ocean backscatter [5].

influenced by the temperature during ice growth and desalination. The surface is composed of melt ponds, hummocks, ice ridges and snow cover with roughness at a range of scales [4]. Scattering from a complex medium like sea ice involves both volume and surface scattering mechanisms. Air bubbles, brine pockets, and snow grains are sources of volume scattering. Because these volume scatterers are randomly oriented or almost spherical, the levels of vertical and horizontal polarization returns,  $\sigma_{vv}$  and  $\sigma_{hh}$ , are thus similar. In other words, the copol ratio  $\sigma_{vv}/\sigma_{hh}$  is near unity for volume scattering. Surface scattering is contributed by the rough surfaces of ice ridges, sea ice and snow cover at all length scales. In general, the surface roughness of sea ice, except thin ice, is comparable with or much larger than the wavelength ( $\sim 2$  cm) of SASS. This means that the geometric optics scattering from surface facets facing the scatterometer may become significant even at large incidence angles. Consequently, the levels of Ku-band  $\sigma_{vv}$  and  $\sigma_{hh}$  will be similar for most sea ice surfaces. From the described characteristics of volume and surface scattering, we anticipate that the copol ratio is close to unity for sea ice at Ku-band, regardless of

which scattering mechanism dominates. Figure 1(a) illustrates the SASS data for two areas, one in the Beaufort sea and the other in the Chukchi sea centered at  $(72^{\circ} 22' 0'' \text{N}, 155^{\circ} 55' 0'' \text{W})$  and  $(72^{\circ}, 190^{\circ})$ , respectively. The size of each area is  $1^{\circ}$  in latitude by  $1^{\circ}$  in longitude. As shown, the copol ratio is less than 2 dB from  $0^{\circ}$  to  $60^{\circ}$  incidence angles, consistent with the physical scattering mechanism described above. The higher backscatter in the Beaufort Sea is probably due to scattering from the more deformed sea ice cover in this region.

The scattering mechanisms of open ocean are quite different from those of sea ice. Sea surfaces roughened by wind forcing are comprised of gravity waves, capillary waves, breaking waves, and foam. The dependence of  $\sigma_{vv}$  and  $\sigma_{hh}$  on the incidence angle and wind speed is illustrated in Figure 1(b) using the SASS 2 model function for upwind observations [5]. The characteristics illustrated here are similar for observations made at other wind directions. The sea surface backscatter is dominated by the Bragg scattering from capillary waves at large incidence angles. The Bragg scattering mechanism provides a unity copol ratio at small incidence angles. However, the copol ratio for Bragg scattering increases with increasing incidence angles and may reach as high as 10 dB at  $60^{\circ}$  incidence at low winds. Figure 1(b) also indicates that the copol ratio of sea surface backscatter depends on wind speed. This might be due to the increasing coverage of breaking waves and foam with increasing wind speed. It has been suggested that breaking waves significantly increase the level of  $\sigma_{hh}$  at high incidence angles in good what is predicted from the Bragg scattering mechanism. An increase in  $\sigma_{hh}$  leads to a reduction of the copol ratio of ocean backscatter. In general, the copol ratio of ocean backscatter increases with increasing incidence angles, unlike that of sea ice.

Comparative analysis of Figures 1(a) and (b) indicates that the backscatter levels from sea ice overlap with the range of backscatter from open water, which depends on wind speeds. This clearly makes it difficult to distinguish sea ice and open water using only backscatter levels. However, the SASS data suggest that the copol ratio for ocean backscatter is larger than that of sea ice backscatter at large incidence angles. To verify whether the above observation is true over a larger area, the copol ratios of the SASS data from the entire polar regions are examined. The ratio of consecutive  $\sigma_{vv}$  and  $\sigma_{hh}$  measurements made by the same antenna beam is calculated for incidence angles between  $43^{\circ}$  and  $58^{\circ}$  and grouped into  $0.5^{\circ}$  by  $0.5^{\circ}$  bins. The results show that the copol ratio is close to 1 (0 dB) for the areas expected to be covered by sea ice and is as large as 5 dB over the open ocean. This supports our conclusion drawn from Figure 1.

### B. Sea Ice/Water Classification Algorithm

The preceding discussion suggests that the copol ratio is a good discriminator of sea ice and open water. Analysis of SASS-2 geophysical model function [5] for several wind speeds shows that the copol ratio for open water is greater than 2 dB at above  $43^{\circ}$  incidence angles for winds up to 20 m/s. Hence, if a value of 2 dB is selected for  $\gamma_t$ , the

threshold algorithm should work rather well for a large range of wind speeds with the backscatter observations at incidence angles greater than  $43^{\circ}$ .

Besides the threshold for copol ratio, the thresholds of backscatter levels are also required to reduce erroneous classification at high and low winds. The copol ratio data for the south polar region show that there will be substantial misclassifications of open water into ice if the copol ratio is used as the only discriminator. The classification can be improved by bracketing the range of backscatter levels. The upper backscatter threshold ( $\sigma_1$ ) is selected to be small enough so that extraordinarily strong wind conditions resulting in high backscatter and small copol ratios will not be confused as sea ice, but is large enough to include as many ice types as possible so that strong backscatter from some winter Antarctic sea ice will not be excluded. The lower threshold ( $\sigma_2$ ) is needed to exclude the noisy backscatter data from open ocean at low winds. We found that the values of 0 dB and -25 dB for  $\sigma_1$  and  $\sigma_2$ , respectively, work well for the summer Arctic and winter Antarctic sea ice with our current data set. Hence, we propose the following algorithm for sea ice and open water discrimination using the data from above  $43^{\circ}$  incidence:

**A pixel is classified as sea ice if**

- $\sigma_{vv}/\sigma_{hh} \leq \gamma_t$ , and
- $\sigma_1 > \sigma_{vv}$  and  $\sigma_{hh} > \sigma_2$ .

**Otherwise, this pixel is classified as open water.**

### APPLICATIONS TO SEASAT DATA

Here, the copol ratio algorithm for sea ice and open water classification is demonstrated with the data from the Seasat scatterometer [3]. SASS used four dual-polarized fan-beam antennas to produce an X-shaped illumination pattern on the earth surface. There were eight science operational modes for beam/polarization scanning. Modes 3 and 4 are single-sided, dual-polarization modes illuminating the left and right sides of the satellite velocity vector, respectively. In early July 1978, SASS operated continuously in mode 4 from revs 142 to 223 with the antenna/polarization scanning sequence (1V, 1H, 2V, 2H). These 82 revs ( $\sim 6$  days) of dual-polarized backscatter data are used to test the sea ice/open water classification algorithm described in the previous section.

The data in the range of incidence angles from  $43^{\circ}$  to  $58^{\circ}$  were averaged and grouped into  $0.5^{\circ}$  latitude and  $0.5^{\circ}$  longitude bins. The copol ratio was calculated from each pair of consecutive  $\sigma_{vv}$  and  $\sigma_{hh}$  measurements from the same antenna beam and averaged over all the SASS observations for each bin. The averaged  $\sigma_{vv}$ ,  $\sigma_{hh}$ , and copol ratio are used to determine whether a bin is sea ice or water. Note that there are bins with no SASS observations from  $43^{\circ}$  to  $58^{\circ}$  incidence angles. For this case, no classification is performed.

The classification results are shown in Figures 2 and 3.  $\sigma_0$  of classified sea ice pixels is indicated with a range of gray levels. As expected in summer, the ice edge is located to the north of the Chukchi sea in the Arctic ocean.

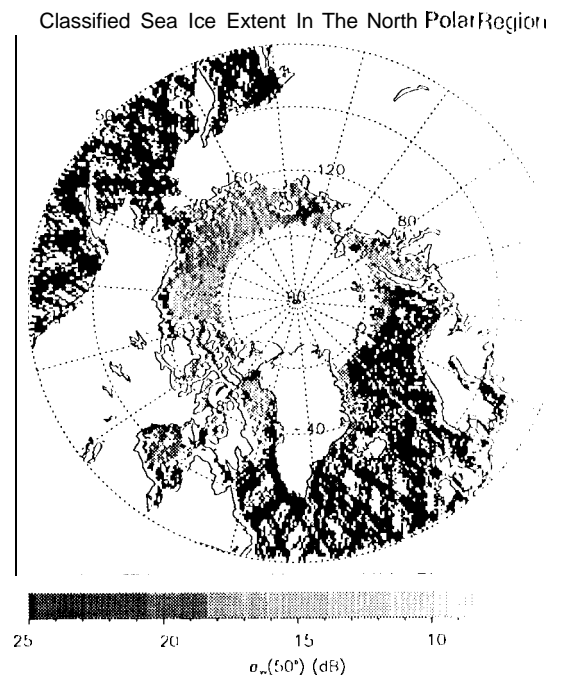


Figure 2. Sea ice backscatter  $\sigma_{vv}$  interpolated at  $50'$  for the north polar regions. Black represents ocean, and white represents land or no data.

A large portion of Baffin Bay was still covered by sea ice, and a large portion of coastal water in the Hudson Bay was open. There was also sea ice off the east Greenland coast. These features agree with the climatological coverage of sea ice in the north polar region [6]. There are only a few obvious misclassifications: A few bins in the north Pacific were classified as sea ice and a few within the ice edge in the Arctic ocean to the north of Chukchi sea classified as open water. For the south polar region, Fig. 3 indicates that the ice edge nearly reached the minimum extent and extended into the mid-latitudes of the south Atlantic, consistent with the climatological ice edge [6]. The clearly identifiable misclassifications are also very limited with very few black pixels well within the ice edge. Although no ground truth information is available to determine the absolute accuracy, the small number of apparent classification errors indicated by the sea ice pixels in the mid-latitude oceans and open water pixels within the ice edges suggests reasonable results from this topological algorithm.

### SUMMARY

A classification algorithm using the dual-polarized radar backscatter is presented for the identification of sea ice cover. This algorithm is demonstrated with the SASS data from the single-sided, dual-polarized modes. A small number of obvious classification errors suggests that this algorithm performs reasonably well for the summer Arctic and winter Antarctic sea ice. Work is being carried out to further reduce these classification errors with the sea ice identification algorithm developed for ERS-1 [1]. If

Classified Sea Ice Extent In The South Polar Region

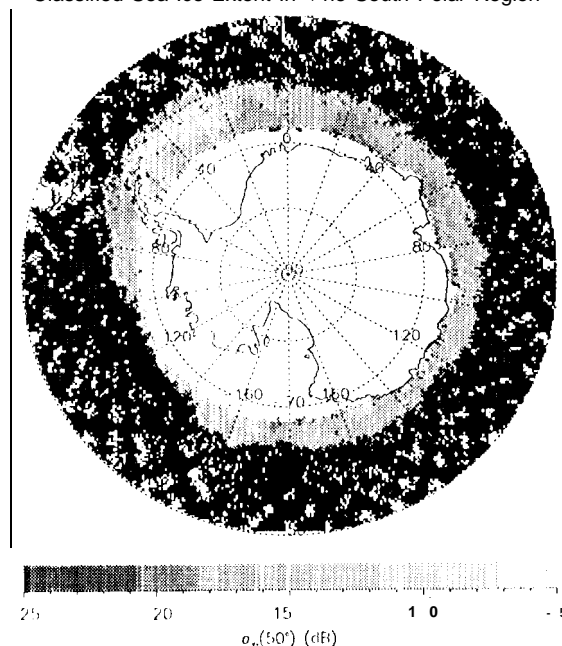


Figure 3. Sea ice backscatter  $\sigma_{vv}$  interpolated at  $50'$  for the south polar regions. Black represents ocean, and white represents land or no data.

this algorithm proves to be useful and accurate for other seasons, the sea ice extent can be produced routinely from the NSCAT data [2] and is expected to complement the current products used for monitoring the extent of sea ice cover.

### REFERENCES

- [1] Golim, F., and A. Cavanic, "A first try at identification of sea ice using the three beam scatterometer of ERS-1," *Int. J. Remote Sensing*, Vol. 15, No. 6, 1221-1228, 1994.
- [2] Nadiri, F. M., M. H. Freilich, and D. G. Long, "Spaceborne Radar Measurement of Wind Velocity Over the Ocean An Overview of the NSCAT Scatterometer System," *Proc. of The IEEE*, Vol. 79, No. 6, 850-866, 1991.
- [3] Boggs, Dale H., *Seasat Geophysical Data Record Users Handbook*, JPL-D 129 (internal document), Jet Propulsion Laboratory, Pasadena, August 1982.
- [4] Tucker, W. B., D. K. Perovich, A. J. Gow, and W. F. Weeks, "Physical properties of sea ice relevant to remote sensing," *Microwave Remote Sensing of Sea Ice*, Frank D. Casey ed., American Geophysical Union, Washington, DC, 1992.
- [5] Wentz, F. J., S. Petcherych, and L. A. Thomas, "A model function for ocean radar cross sections at 14.6 GHz," *J. Geophys. Res.*, Vol. 89, No. C3, 3689-3704, 1984.
- [6] Gloersen, P., D. J. Cavalieri, J. Comiso, C. L. Parkinson, and H. J. Zwally, *Arctic and Antarctic Sea Ice, 1978-1987: Satellite Passive Microwave Observations and Analysis*, *Electromagnetics*, NASA Spec. Publ., SP-511, 289 pp, 1992.